~~RESTRICTED~~

NACA

RESEARCH MEMORANDUM

EFFECTS OF TWIST AND CAMBER ON THE LOW-SPEED CHARACTERISTICS OF A LARGE-SCALE 45° SWEPT-BACK WING

By Lynn W. Hunton

Ames Aeronautical Laboratory
Moffett Field, Calif.

NATIONAL ADVISORY COMMITTEE FOR AERONAUTICS

WASHINGTON

March 20, 1950

~~RESTRICTED~~

NATIONAL ADVISORY COMMITTEE FOR AERONAUTICS

RESEARCH MEMORANDUM

EFFECTS OF TWIST AND CAMBER ON THE LOW-SPEED CHARACTERISTICS OF A LARGE-SCALE 45° SWEPT-BACK WING

By Lynn W. Hunton

SUMMARY

An investigation has been conducted to determine the effects of camber and twist on the low-speed aerodynamic characteristics of a large-scale, semispan, wing-fuselage model with the 0.25 chord line of the wing swept back 45°. Force tests, tuft studies, and pressure-distribution measurements were obtained on two models, both having an aspect ratio of 6 and a taper ratio of 0.5, one uncambered and untwisted and the other cambered and twisted for an ideal lift coefficient of 0.4.

Results of the tests revealed that a significant improvement in the low-speed performance of highly swept thin wings can be achieved through the use of an amount of camber and twist indicated by theory to be also desirable from a high-speed standpoint. Flow separation on the wing was delayed from a lift coefficient of 0.65 (69 percent of $C_{L_{max}}$ of the uncambered, untwisted wing) to 1.07 (98 percent of $C_{L_{max}}$ of the cambered, twisted wing). The point of initial separation was moved inboard away from the critical tip region. The stall of the wing at maximum lift was changed from a gradual type for the uncambered, untwisted wing to a rather abrupt type which occurred over a large area of the cambered, twisted wing. A decrease in lift-curve slope and a nose-up tendency, both of which occurred near maximum lift of the cambered, twisted wing, are believed to be attributable to the behavior of the boundary-layer air. A comparison of theoretical span loadings and associated aerodynamic characteristics with the experimental data for both wing models showed satisfactory agreement.

INTRODUCTION

It is commonly accepted that large improvements in the performance of aircraft at high subsonic and supersonic speeds are possible through the use of wing sweep. Results of theoretical wing-loading studies have

indicated that still further gains in the performance of swept wings in the high-speed range could be achieved by distributing the loading over the wing uniformly spanwise and chordwise. The most direct means of achieving this end appears to be the use of twist and camber. Wing twist would serve the dual purpose of assuring constant spanwise section lift (critical speed not prematurely reached at local wing points) and minimum induced drag. Section camber would distribute the load chordwise and avoid high negative pressures at the leading edge. In addition to these anticipated gains at high speed, the study of the problem has indicated that such twist and camber also should improve significantly the low-speed characteristics of thin swept-back wings. The redistribution of spanwise loading resulting from twist should relieve the highly loaded tip and the camber should delay the leading-edge separation typical of thin sections.

References 1 and 2 provide a means of determining the twist distribution required to obtain a desired span load distribution on swept wings. Ample two-dimensional theory and experimental data exist to define a desired camber line. It is thus possible to determine the required twist and camber of a swept wing which presumably will give improved characteristics when compared to a swept wing of similar plan form which is neither cambered nor twisted. This report compares the characteristics of two such wings as determined in the Ames 40- by 80-foot wind tunnel at a test Reynolds number of 8 million.

NOTATION

The data are presented in the form of standard NACA coefficients which are applicable to a full-span configuration. Moments are referred to the quarter-chord point of the mean aerodynamic chord[1] (fig. 1) and all coefficients are based on the dimensions[2] of the untwisted wing.

C_L lift coefficient $\left(\frac{L}{qS}\right)$

C_D drag coefficient $\left(\frac{D}{qS}\right)$

C_{D_i} induced drag coefficient

C_m pitching-moment coefficient $\left(\frac{M}{qS\bar{c}}\right)$

[1]The mean aerodynamic chord is located in the wing reference plane defined by the quarter-chord line of the wing panel and the root chord line at the axis of symmetry.

[2]The projected area of the twisted wing at 0° angle of attack of the wing-root section was approximately 0.5 percent less than the area of the untwisted wing.

C_{m_o} pitching-moment coefficient at zero lift

c_l section lift coefficient

c_{m_o} section pitching-moment coefficient at zero lift

A aspect ratio $\left(\frac{b^2}{2S}\right)$

D drag on semispan wing

L lift on semispan wing

M pitching moment of semispan wing

M_{cr} critical Mach number

R Reynolds number

S area of semispan wing

b span of complete wing, feet

$\bar{c}$ mean aerodynamic chord $\left(\frac{\int_o^{b/2} c^2 dy}{\int_o^{b/2} c\, dy}\right)$, feet

c local chord measured parallel to plane of symmetry, feet

q dynamic pressure, pounds per square foot

y spanwise coordinate normal to plane of symmetry, feet

α angle of attack of wing reference plane, degrees

α_{L_o} angle of attack for zero lift

ϵ angle of twist with respect to root chord (positive for washin), degrees

η dimensionless lateral coordinate $\left(\frac{y}{b/2}\right)$

THEORY

To properly evaluate the advantages and/or disadvantages of the camber and twist combination considered in this report, it is necessary to be cognizant of the factors governing the design of the wing and of the gains to be expected in the case of this particular design.

The first choice of the values of the geometric parameters of a wing design would, of course, be made on the basis of high cruising speed considerations with a view to achieving minimum drag for a given lift within structural limitations. For flight near sonic speeds, experiment has shown that large sweep angles are required if high drags are to be avoided. Theory and experiment both show, however, that sweep distorts the load distribution such that the desirable minimum induced drag is not achieved and, with normal tapers, the section lift coefficients vary widely so that section critical speeds are reached at some spanwise stations far earlier than at others. The extent to which these unfavorable effects are encountered increase with wing aspect ratio and with lift coefficient. If twist and camber can improve wing characteristics, then it appears they will be of major importance on a wing of high aspect ratio operating at a relatively high lift coefficient at the cruise condition such as is normally encountered on the airplane of the transport or bomber type. Accordingly, this reasoning was used as a basis for the design of the wings the characteristics of which are reported herein.

A sweep angle of 45° was chosen as a value believed to be consistent with current considerations of the speeds of large airplanes. An aspect ratio of 6 combined with a taper ratio of 0.5 was chosen to obtain approximately elliptic spanwise distribution of load when the twist required for constant spanwise distribution of section lift coefficient was introduced. A design lift coefficient of 0.4 was chosen, this being slightly higher than commonly used. However, it was believed only small penalties would result at very low lift coefficients; whereas significant gains would result in the moderate to high lift coefficient range. Based on the concepts of simple sweep theory, the airfoil sections were laid out normal to the quarter-chord line. The NACA 64A010 thickness distribution was chosen on the basis both that it was typical from a high-speed standpoint and that the maximum thickness of 10 percent fitted the criterion that a ratio of wing length to wing-root thickness of 50 is structurally feasible. The wing design lift coefficient of 0.4 (based on the free-stream velocity) requires a section lift coefficient of 0.8 (based on the velocity perpendicular to the quarter-chord line in accordance with the concept of simple sweep theory); thus, the section used was an NACA 64A810.

Design of the twist distribution in the wing entailed considerations not only of aerodynamics but of fabrication problems as well. In references 1 and 2, a procedure based on the Weissinger method is outlined for the determination of the twist distribution for any arbitrary span loading. The required twist distribution, computed by this method for a uniform spanwise section lift coefficient c_l of 0.4, is shown in figure 2.

It may be noted that the theory indicates that a large untwisting (washin) of the tip is necessary to carry the loading uniformly to the tip. Such a twist distribution appeared undesirable from two standpoints. First, experiments with finite aspect ratio wings have shown the impossibility of carrying a uniform load to the wing tip. Second, construction of a wing having such a twist distribution would require extensive use of doubly curved surfaces. It was concluded, therefore, that a compromise twist distribution should be chosen.

From purely structural considerations the optimum twist variation would be one which resulted in straight line elements spanwise along any constant percent-chord line. In this case only single curvature would be required for contouring such a wing, thereby greatly facilitating the construction. For a tapered wing the resultant spanwise variation of twist for straight line elements is nonlinear, the rate of change of twist with span increasing along the span. For the wing under consideration, the twist is as shown in figure 2.

The theoretical spanwise distributions of c_l are also shown in figure 2 for the wing having the straight-line-element type of twist with 10° of washout at the tip and for the same wing with no twist, each computed by the method of references 1 and 2 for a wing ideal lift coefficient of 0.4. It should be noted that, insofar as increasing the critical speed, the compromise twist is only slightly effective. The peak c_l (presumably indicative of M_{cr}) of the untwisted wing is 19 percent above the average c_l of 0.4, while the peak c_l of the twisted wing is about 16 percent above. However, it is evident that the peak c_l is moved far inboard (from $\eta = 0.7$ to $\eta = 0.33$) which, it could be expected, would reduce tip-stall tendencies both directly and because the spanwise boundary-layer flow would be restrained by the rising spanwise pressure gradient. To illustrate the magnitude of these effects at higher lift coefficients, the spanwise distributions of c_l for the two wings are also shown in figure 2 for a wing lift coefficient of 1.0. From these results, too, it would be anticipated that the use of this twist would delay tip stall. It is of interest that the load distribution of the wing having the compromise twist (i.e., the straight-line-element twist) approaches that recommended in reference 3 for optimum stalling characteristics.

With a view to improving M_{cr}, wings having smaller amounts of the compromise twist were considered to determine whether the peak c_l could be reduced at a wing C_L of 0.4. It was found that the reduced twist served only to move the spanwise position of the peak c_l outboard. Furthermore, at a wing C_L of 1.0, the peak c_l was not only moved outboard but increased as well. Hence, in view of the apparent advantages from such a constructionally simple wing in the way of a more readily attainable type of load distribution as compared with the ideal uniform c_l distribution and, in view of the prospects of significant improvements in the low-speed characteristics, the twist variation shown in figure 3 was incorporated in the cambered, twisted wing.

MODELS AND APPARATUS

The principal dimensions of the two semispan wing–fuselage models used in the investigation are shown in figure 1. Except for twist and camber, the two models were identical. The wings had a sweepback angle of the quarter–chord line of 45°, an aspect ratio of 6, a taper ratio of 0.5, and no dihedral. Both wings had the NACA 64A010 profile thickness distribution normal to the quarter–chord line. One wing model, hereinafter called the plain wing, had no twist and no camber. The second wing model had both twist and camber.

The spanwise twist, shown in figure 3, was a straight–line–element type wherein all constant-percent–chord points along the span lie in straight lines. The quarter–chord line was used as a reference axis about which all sections were twisted. In this manner the airfoil sections normal to the quarter–chord line remained true and undistorted. The twist distribution shown in figure 3 is based on the angle of twist of the streamwise section chord line through the leading– and trailing–edge points. This twist varied from 0° at the root section to −10° (washout) at the tip.

The camber was uniform along the span and consisted of an $a = 0.8$ type mean line (modified as shown in reference 4) cambered for an ideal section lift coefficient of 0.8. Thus, for the cambered, twisted wing the sections normal to the quarter–chord line were the NACA 64A810. The section coordinates for both wing models are given in table I.

Both wings were constructed of laminated mahogany over a steel framework. The wings were lacquered and sanded to approach an aerodynamically smooth surface.

The fuselage used for both wing models had a fineness ratio of 4.9 and consisted of half of a body of revolution with a cylindrical midsection as shown in figure 1. For both wing–body combinations, the wing–root chord line was coincident with the longitudinal axis of the fuselage.

Each wing was equipped with 440 pressure orifices distributed over the upper and lower surfaces at 6 stations oriented parallel to the axis of symmetry and at 5 stations oriented normal to the quarter–chord line.

As shown in figure 4, the models were mounted vertically on the tunnel test–section floor which served as a reflection plane for this semispan arrangement. The models were supported on a turntable, independent of the tunnel–floor structure, in such a manner that only the aerodynamic forces and moments on the wing–fuselage combination were measured on the tunnel six–component balance system.

TESTS

Force, pressure-distribution, and tuft-study tests were made on both models through an angle-of-attack range from -2° to the stall angle. All tests reported herein were performed at a Reynolds number of 8 million based on a wing mean aerodynamic chord of 6.21 feet. This corresponds to a dynamic pressure of about 55 pounds per square foot and a Mach number of 0.2.

The following jet-boundary corrections derived from reference 5 for an unswept semispan wing installation were added to the angle-of-attack and drag-coefficient data:

$$\Delta\alpha = 0.26\, C_L$$

$$\Delta C_D = 0.0045\, C_L^2$$

No corrections were made for the effect of the boundary-layer air on the tunnel floor (reflection plane) or for the leakage through the clearance gap (1/4 inch) between the fuselage and the tunnel floor. Measurements of the total thickness of the boundary layer on the tunnel floor (at the model location) and on top of the fuselage (near the leading edge of the wing) revealed the thicknesses to be of the order of 14 inches and 1 inch, respectively, for the test conditions of this investigation.

RESULTS AND DISCUSSION

Lift and Stalling Characteristics

The longitudinal aerodynamic characteristics for both wing models are presented in figure 5. It may be seen that the effect of the camber and twist on the angle of attack for zero lift α_{L_o} was quite small. This result may be partially explained as follows. The theoretical angle of attack for zero lift of the NACA 64A810 section is -6.2°. Correcting this value for the effect of sweep ($-6.2^\circ \times \cos 45^\circ$) gives an approximate value for α_{L_o} of -4.4° due to camber. Computations of the effect of the wing twist on α_{L_o} (by method of reference 2) indicate a positive incidence of 2.9°. The combination of these two counter effects, camber and twist, gives a theoretical α_{L_o} value of -1.5° as compared with the measured value of -0.3°.

The slopes of the lift curve of the plain wing and the cambered, twisted wing at zero lift are 0.059 and 0.060, respectively. A computed value of 0.058 by the Weissinger method compares favorably with the experimental results.

The camber and twist of the wing increased the value of $C_{L_{max}}$ from 0.94, measured for the plain symmetrical wing, to 1.09 and altered the well rounded lift curve of the plain wing at the stall to a moderately abrupt type. In the case of either wing it may be noted that a decrease of lift-curve slope began at a lift coefficient of about 0.65. However, the stalling characteristics of the two wings were very dissimilar, although it was not apparent from the force test results. This may be seen in figure 6 in which are presented tuft-study photographs for both wing models throughout the angle-of-attack range. For the plain wing, the familiar stall progression for conventionally tapered, thin, swept-back wings which begins at the tip and extends inboard with increasing angle of attack is clearly evident in figure 6(a). The first evidence of flow separation[3] at the tip indicated by these photographs occurs at a lift coefficient of about 0.7, while at the angle of attack for maximum lift nearly the entire wing surface shows evidence of flow separation. Hence, the $C_{L_{max}}$ of 0.94 of the plain wing may be considered equivalent to the maximum lift of a flat plate with full separation of flow from the leading edge entailing high values of drag as is evident from the measured force data shown in figure 5 for this wing.

In contrast to this stalling behavior of the plain wing, the tuft photographs of the cambered, twisted wing show no evidence of separation until $C_{L_{max}}$ is nearly reached. Thus, the anticipated gains (regarding premature separation) on this wing were closely realized. The maximum value of lift coefficient entailing no separation was increased by the camber and twist from about 0.7 to 1.07. It is not known at this time, however, in what proportions this increase in C_L may be attributed to the camber or to the twist. A close observation of the tuft behavior during the tests indicated that at a lift coefficient of 1.07 a small stalled area appeared momentarily at the trailing edge of the wing near the midpoint of the semispan and was followed immediately by an abrupt stall over a large area of the wing both inboard and outboard of this point.

The tuft-study results give no clue to an explanation for the gradual reduction in lift-curve slope of the cambered, twisted wing that occurred in the lift-coefficient range from about 0.65 to $C_{L_{max}}$. From a preliminary analysis of the pressure data obtained on the wing, it is believed that this reduction in slope is attributable to losses in lift which occurred over the outboard 0.6 of the wing semispan. These reductions in lift, which were greatest at the tip, are believed to result from a thickening of the boundary layer over the after part of the affected wing sections presumably due to the spanwise drainage of the boundary-layer air.

[3] Separation defined by violent motion of tufts.

Pitching-Moment Characteristics

A comparison of the pitching-moment-coefficient variation with lift coefficient for the two wing models is included in the force data of figure 5. The stability of the plain wing was quite uniform up to a lift coefficient of about 0.55 with an aerodynamic center located at 0.26 mean aerodynamic chord. Above a lift coefficient of 0.55 the stability of the wing momentarily increased then reversed, giving a strong nose-up tendency with increasing lift coefficient. The slight increase in stability probably resulted from the formation of a laminar-separation bubble near the leading edge of the highly loaded tip, which is characteristic of relatively thin sections with a small leading-edge radius. This would shift the section center of pressure to the rear but would not seriously reduce the lift. The unstable nose-up tendency that occurred above a lift coefficient of 0.65 may be accounted for as resulting from the separation of flow and consequent loss of lift at the tip of the wing which was described previously in connection with the tuft study.

The principal effects of the camber and twist on the stability of this wing plan form may be seen to be: (1) a marked increase in stability at lift coefficients below 0.1; (2) a shift in the value of C_{m_o} to a small negative value; (3) no change in the horizontal position of the aerodynamic center although a small change in vertical location; (4) an increase of the lift coefficient from about 0.65 to 0.80 at which the pitching-moment curve indicates stability; and (5) a tendency toward instability of the wing in the upper lift-coefficient range which occurs at a lift coefficient considerably lower than that at which the tuft studies indicate any significant amount of flow separation.

Based on observations of tufts on the lower surface, the stable slope of the pitching-moment curve near zero lift coefficient resulted from the separation of flow from the lower surface near the leading edge of the outboard sections which, at low lift coefficients of the wing, were operating at negative angles of attack. It would be expected, however, that this condition, which would be unsatisfactory for flight at the lower lift coefficients, would be alleviated in a wing design involving either a lesser amount of camber and/or twist of the type employed on the subject wing model or a different twist distribution approaching more nearly the ideal type indicated by theory.

Extending the pitching-moment curve of the cambered, twisted wing to the zero-lift axis by neglecting the highly stable portion of the curve indicates a pitching-moment coefficient at zero lift C_{m_o} of about -0.015. The theoretical two-dimensional value of c_{m_o} for the NACA 64A810 section is approximately -0.16, which when adjusted for the effect of sweep ($c_{m_o} \times \cos^2 45^\circ$), results in a C_{m_o} of the wing of -0.08 due to camber. The C_{m_o} resulting from the basic loading on the twisted wing (computed by the Weissinger method, references 1 and 2) is 0.08.

Thus, based on these theoretical considerations the two counter effects would be expected to nullify each other, resulting in a zero value for C_{m_o} of the wing. The discrepancy between this theoretical value and the extrapolated value of −0.015 for C_{m_o} probably results from a combination of effects such as: (1) the influence of the fuselage on the wing loading; (2) the rearward shift of the center of pressure known to occur on sections lying near the root of a swept-back wing; and (3) the inadequacy of the simple sweep theory when applied to wings of finite span.

In the lift-coefficient range from 0.1 to 0.8, the pitching-moment curve, although relatively free from irregularities, is slightly parabolic based on a moment center located on the mean aerodynamic chord line. The aerodynamic center, therefore, while it remained at the same $0.26\bar{c}$ longitudinal location as measured on the plain wing, was displaced below the wing-reference plane (approximately $0.05\bar{c}$) as a result of the large camber of the section. The aerodynamic-center location predicted by the Weissinger method for the wing alone is $0.29\bar{c}$. If it is assumed that this predicted value is accurate for the wing alone, it is indicated that there was a forward shift of the aerodynamic center of about $0.03\bar{c}$ attributable to the fuselage. This does not agree, however, with the theoretical work of Schlichting in reference 6 wherein the influence of a fuselage on a 45° swept-back wing is indicated to be a rearward shift of the aerodynamic center of approximately 0.02 to $0.03\bar{c}$.

Above a lift coefficient of 0.8, the pitching-moment curve indicates increasing instability of the wing up to maximum lift. Although concrete evidence for a full explanation of this trend is lacking at the present time, it appears to be associated with the same losses in lift and attendant variation of location of the center of pressure that resulted in the reduced lift-curve slope over the high-lift range.

Drag Characteristics

Comparisons of the drag characteristics of the two wing-fuselage models are given in figures 5, 7, 8, and 9. In figure 5, the results indicate a minimum drag coefficient for the plain wing-fuselage model at zero lift of 0.0095 as compared with a minimum drag coefficient value for the cambered, twisted model of 0.0145 at a lift coefficient of about 0.13. At the design lift coefficient of 0.4, the drag coefficient of the cambered, twisted wing may be seen to be 0.0190; whereas the drag coefficient of the plain wing has increased to 0.0215. The principal effect of the camber and twist on the drag characteristics is evident in the value of the lift coefficient at which the drag starts to increase rapidly. For the plain wing, the abrupt drag increase starts at a lift coefficient of about 0.65 coincident with the initial occurrence of separation on the tip; whereas for the cambered, twisted wing the force data show no abrupt increase in drag coefficient until the $C_{L_{max}}$ is reached. The effect of

this large improvement in the drag polar on the performance of the wing in the low-speed range may be seen in the comparisons of the lift-drag ratio (fig. 7) and power-off gliding characteristics (fig. 8). The camber and twist increased the value of $(L/D)_{max}$ from 18.7 to 20.2 which for both wings occurred at a lift coefficient of about 0.4. At the respective maximum lift coefficients of each of the wings the value of L/D was approximately 3 for the plain wing as compared with 11 for the cambered, twisted wing. In figure 8, the drag data from figure 5 have been reproduced to show the effect of the camber and twist on the power-off gliding characteristics of the wing without flaps. The computations are based on a wing loading of 50 pounds per square foot. The improvement in the lift-drag ratio in the low-speed range due to the camber and twist resulted in a reduction in the gliding speed from about 170 to 135 miles per hour at a sinking speed of 18 feet per second.

In figure 9 is shown a comparison between the induced drag coefficient of the two wings plotted as a function of C_L^2 and the theoretical variation of the induced drag coefficient computed for both wings by the Weissinger method. For purposes of this comparison, which pertains to only the slopes of the curves, an approximate value for the profile-drag coefficient of 0.0100 was deducted from the experimental drag data for each of the wing models. As a reference to gage the efficiency of the wings indicated by either experiment or theory, a curve showing the ideal slope dC_{D_i}/dC_L^2 corresponding to the value of $1/\pi A$ for a wing with elliptic loading is also given in figure 9. For both wing models, it may be noted that the efficiencies indicated by the theoretical results are generally too high compared with the experimental data.

Span Loading Characteristics

To illustrate the accuracy of the Weissinger method for predicting the span loading, basic as well as additional, a comparison is shown in figure 10 of the experimental data with the spanwise c_l distribution computed by this method for a wing lift coefficient of 0.4. The experimental data were obtained from integrations of the section pressure distributions measured on the plain wing and on the cambered, twisted wing. It may be seen that, while some discrepancy between the theoretical and experimental results exists in the case of the plain wing (approximately 8 percent maximum), for the cambered, twisted wing very good agreement is shown. Thus, it would appear from this result that on wings where poor flow conditions exist, such as on the plain wing, the accuracy of the theoretical span-loading method is reduced.

CONCLUDING REMARKS

Based on the results of this investigation it may be concluded that by use of an amount of twist and camber, theoretically consistent with the requirements of high speed, significant improvements can be made in the low-speed performance of highly swept, thin wings. It is possible by means of twist and camber to not only postpone the initial occurrence of separation, but also to move the point at which stall first appears on a swept-back wing away from the critical tip region to a midsemispan position. It is difficult to prevent inboard separation at one point on a swept-back wing from immediately stalling all sections outboard of this point. The behavior of the boundary layer on highly swept wings appears to be the major factor contributing to large changes in section characteristics across the span. Below the point of initial separation,the Weissinger method for predicting span loading and associated aerodynamic characteristics for both the basic and additional types of loadings appears to give satisfactory results for most normal preliminary design requirements. The two-dimensional-section theory seems adequate to predict the section characteristics on swept wings except in the immediate vicinity of the root and tip.

A sound judgment regarding the over-all advantages of an application of large amounts of camber and twist on highly swept wings necessarily must await results of an investigation of the general aerodynamic characteristics of such wings at high speeds.

Ames Aeronautical Laboratory,
National Advisory Committee for Aeronautics,
Moffett Field, Calif.

REFERENCES

1. DeYoung, John: Theoretical Additional Span Loading Characteristics of Wings With Arbitrary Sweep, Aspect Ratio, and Taper Ratio. NACA TN 1491, 1947.

2. Stevens, Victor I., Jr.: Theoretical Basic Span Loading Characteristics of Wings With Arbitrary Sweep, Aspect Ratio, and Taper Ratio. NACA TN 1772, 1948.

3. Anderson, Raymond F.: A Comparison of Several Tapered Wings Designed to Avoid Tip Stalling. NACA TN 713, 1939.

4. Loftin, Laurence K., Jr.: Theoretical and Experimental Data for a Number of NACA 6A-Series Airfoil Sections. NACA TN 1368, 1947.

5. Glauert, H.: The Elements of Aerofoil and Airscrew Theory. The Macmillan Company, N. Y., 1943.

6. Schlichting, H.: Calculation of the Influence of a Body on the Position of the Aerodynamic Centre of Aircraft With Sweptback Wings. TN Aero 1879, R.A.E. (British), Mar. 1947.

TABLE I.- COORDINATES OF THE AIRFOIL SECTIONS

[Stations and ordinates given in percent of airfoil chord.]

NACA 64A010	
Station	Ordinate
0	0
.5	.804
.75	.969
1.25	1.225
2.5	1.688
5	2.327
7.5	2.805
10	3.199
15	3.813
20	4.272
25	4.606
30	4.837
35	4.968
40	4.995
45	4.894
50	4.684
55	4.388
60	4.021
65	3.597
70	3.127
75	2.623
80	2.103
85	1.582
90	1.062
95	.541
100	.021
L.E. radius = 0.687	
T.E. radius = 0.023	

TABLE I.- CONCLUDED.

[Stations and ordinates given in percent of airfoil chord.]

NACA 64A810 (a = 0.8 modified)			
Upper surface		Lower surface	
Station	Ordinate	Station	Ordinate
0	0	0	0
.214	.976	.785	−.526
.428	1.231	1.072	−.597
.881	1.650	1.619	−.686
2.064	2.475	2.936	−.787
4.506	3.716	5.494	−.832
6.984	4.703	8.016	−.811
9.479	5.541	10.521	−.771
14.500	6.902	15.500	−.658
19.543	7.968	20.457	−.526
24.601	8.795	25.399	−.383
29.668	9.420	30.332	−.232
34.742	9.857	35.258	−.065
39.820	10.107	40.180	.123
44.900	10.150	45.100	.364
49.977	10.005	50.023	.637
55.049	9.693	54.951	.917
60.114	9.225	59.886	1.187
65.169	8.612	64.831	1.426
70.215	7.850	69.785	1.610
75.252	6.932	74.748	1.710
80.300	5.819	79.700	1.657
85.292	4.441	84.708	1.331
90.204	3.004	89.796	.920
95.104	1.512	94.896	.450
100.000	.021	100.000	−.021
L.E. radius = 0.687 T.E. radius = 0.023			

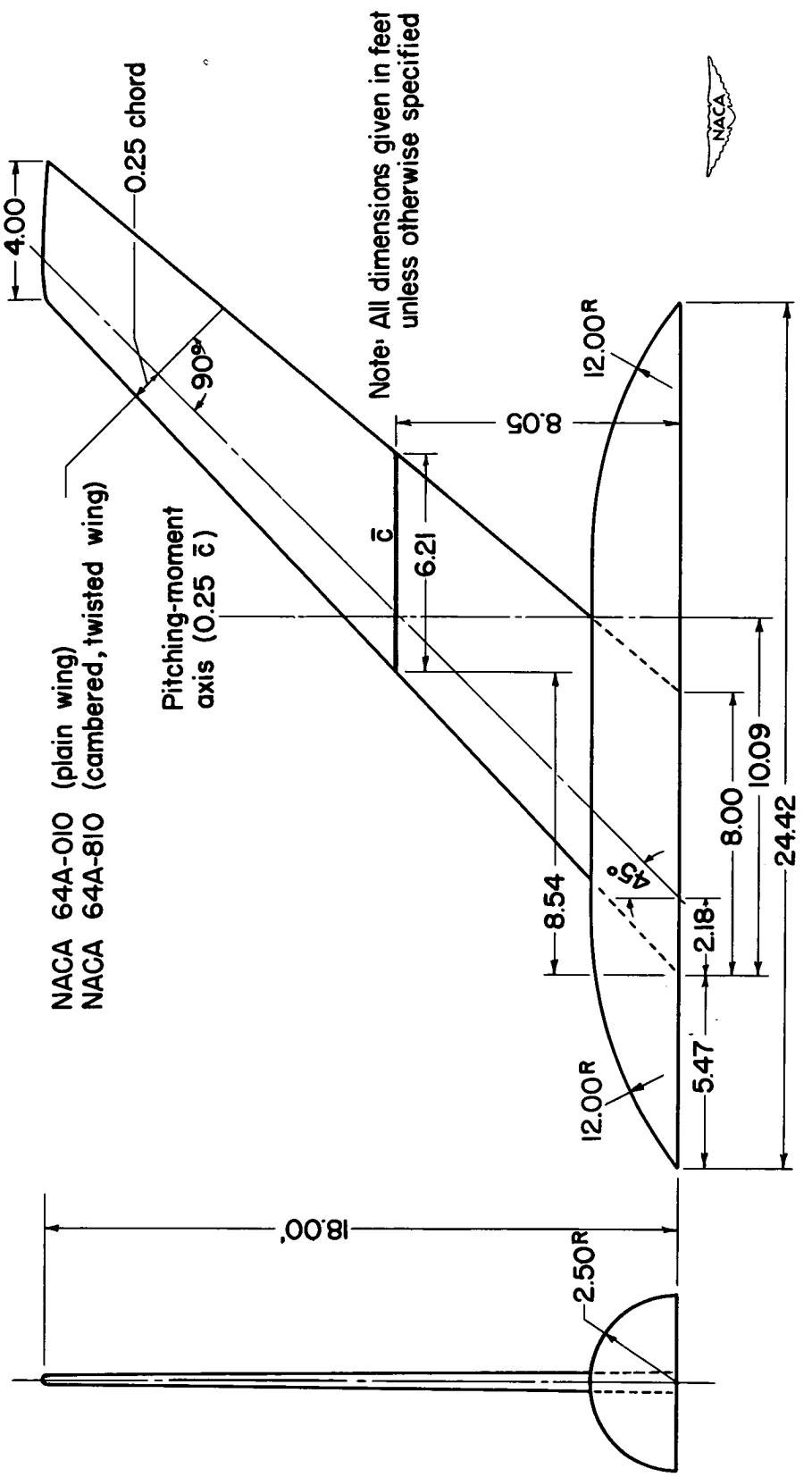

Figure 1.- Dimensions of the semispan wing-fuselage models.

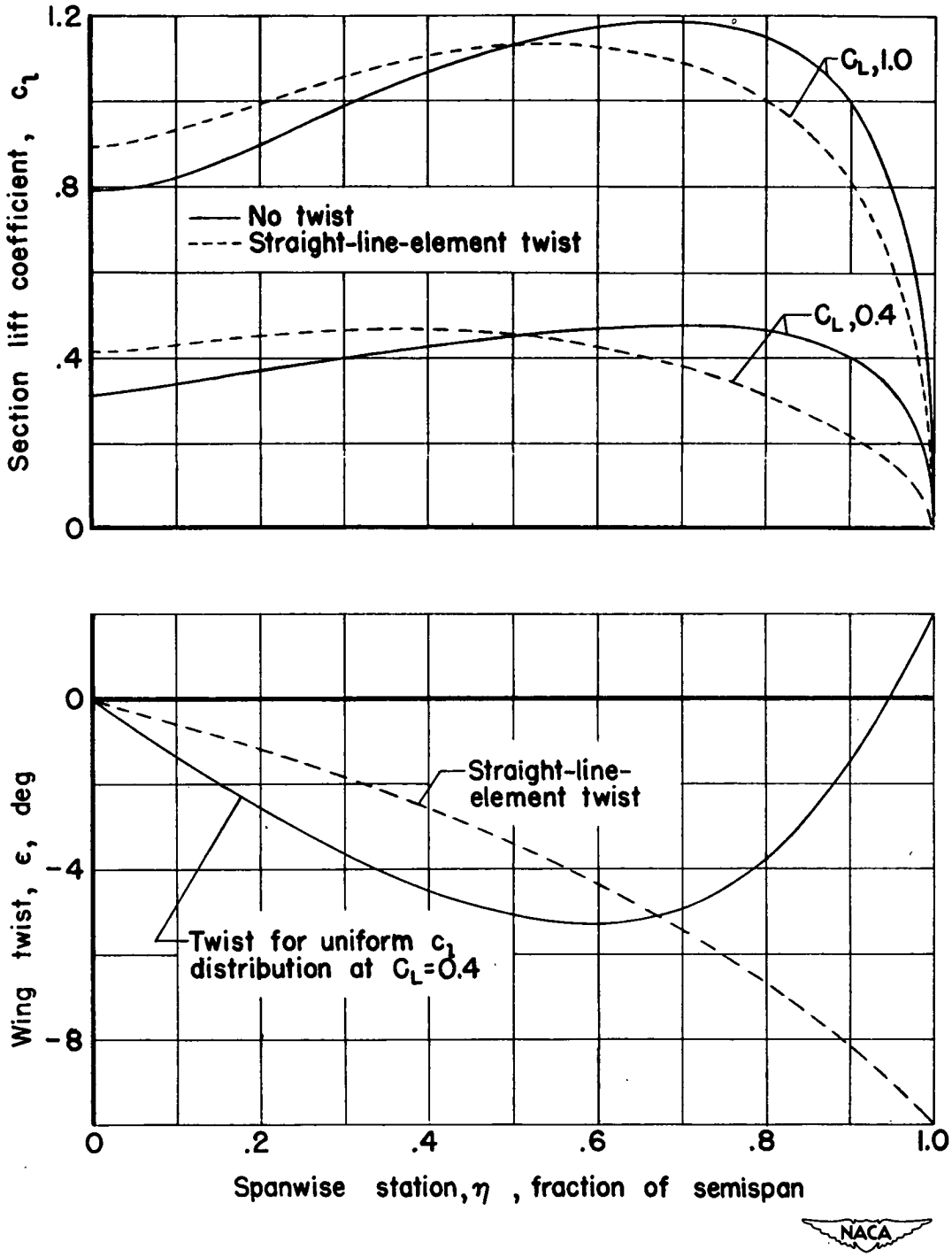

Figure 2.- Comparisons of theoretical spanwise variations of wing twist and distributions of section lift coefficient.

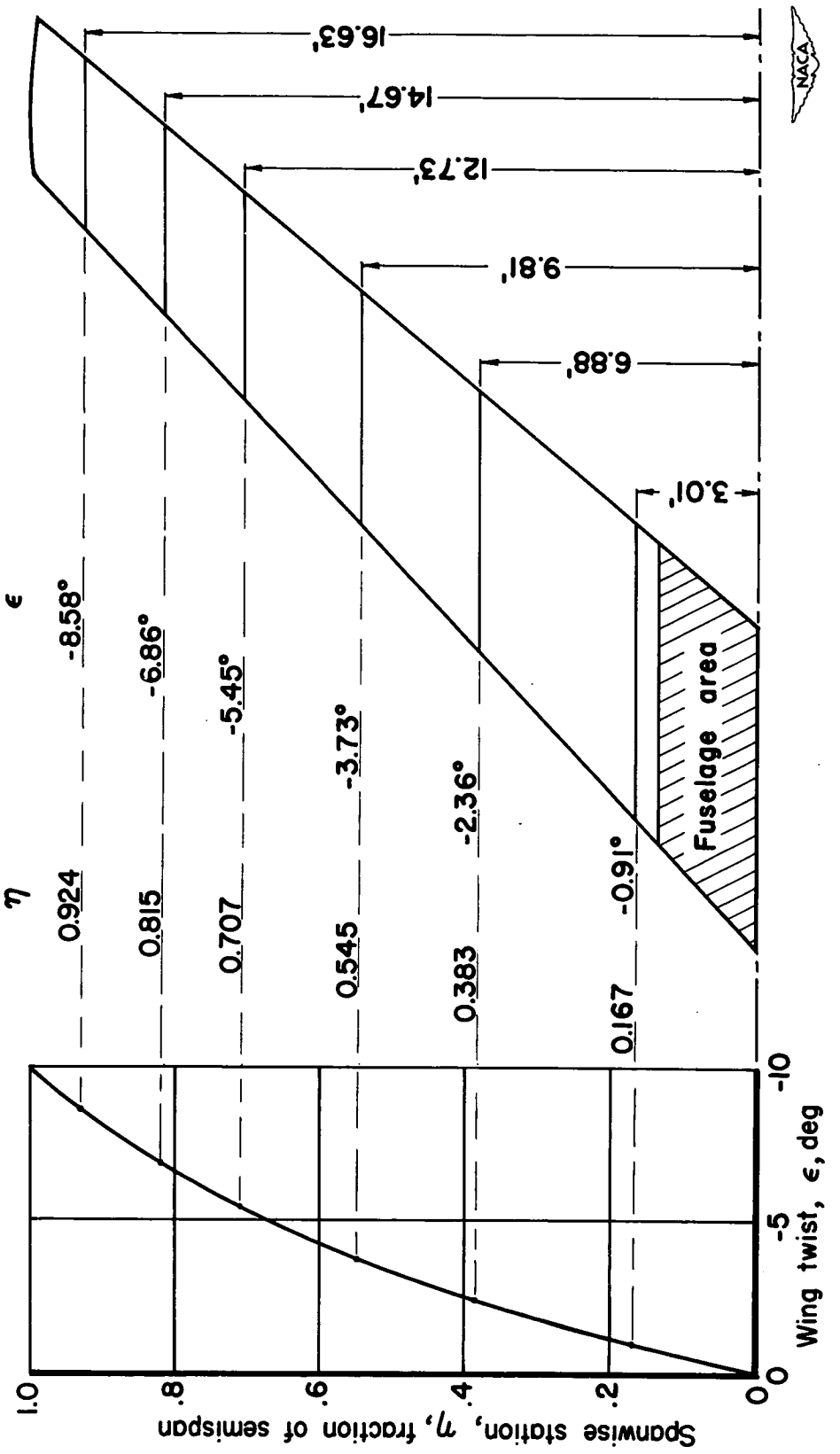

Figure 3.- Variation of twist on the cambered, twisted wing.

Page intentionally left blank

Page intentionally left blank

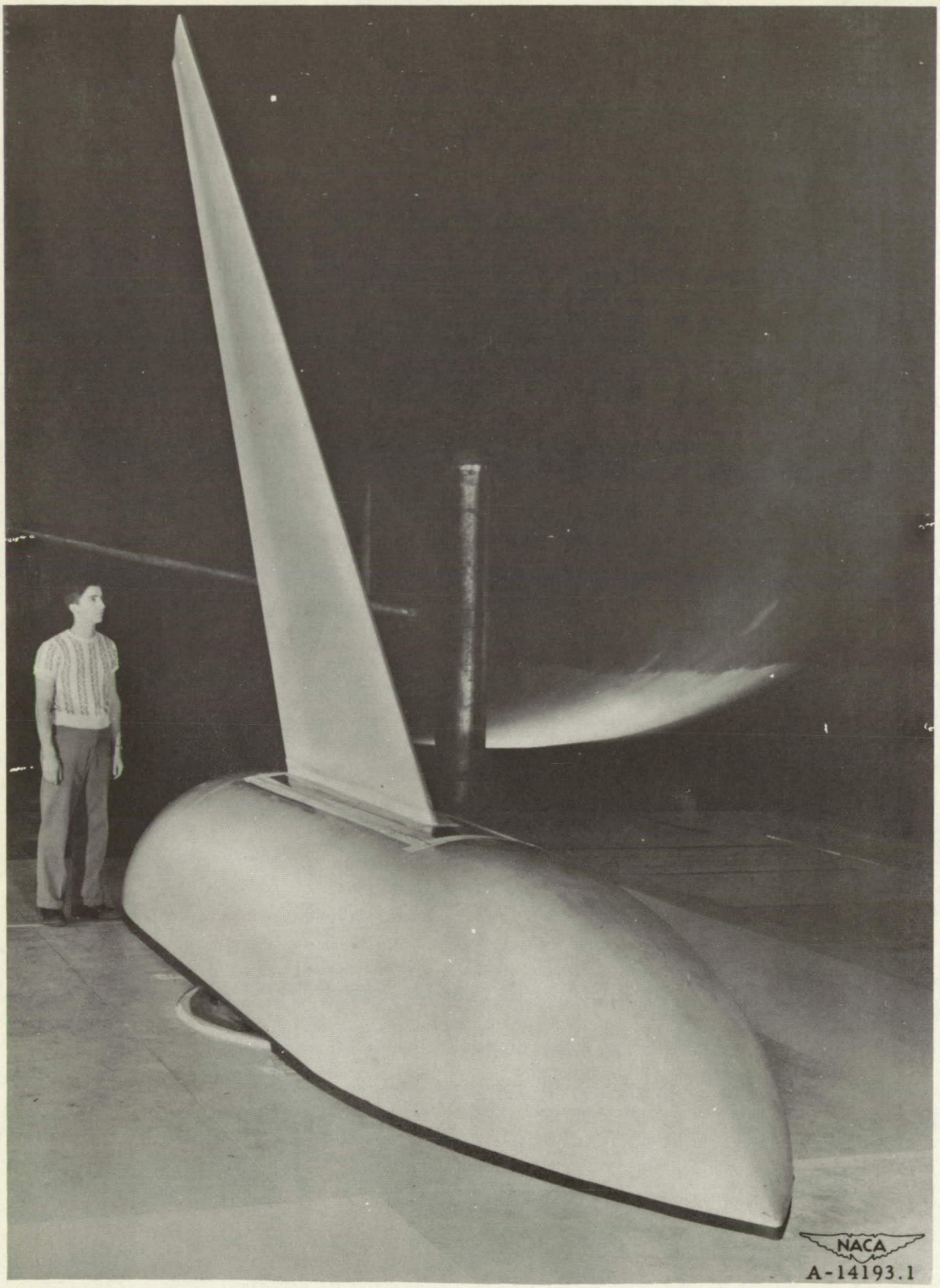

Figure 4.– Three–quarter front view of the semispan installation of the cambered, twisted–wing–fuselage model in the Ames 40– by 80–foot wind tunnel.

Page intentionally left blank

Page intentionally left blank

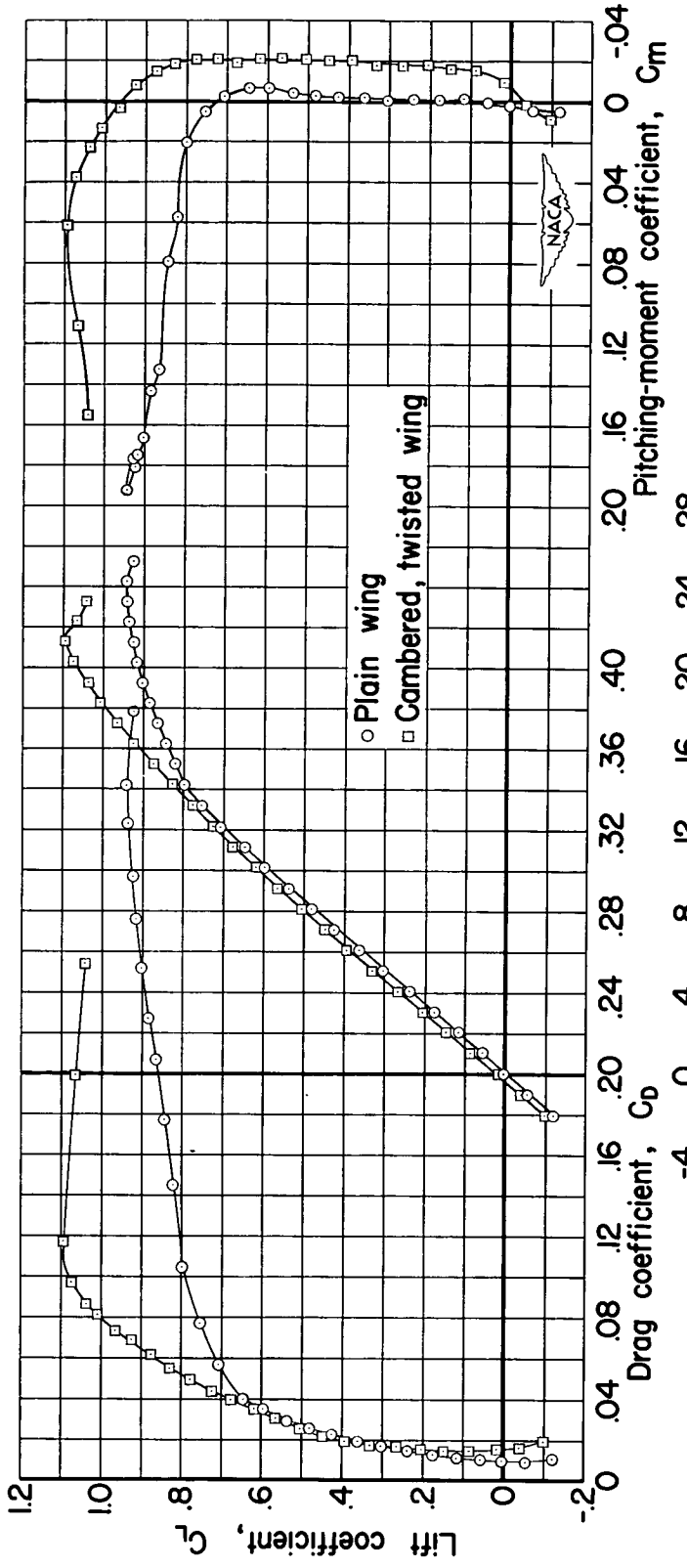

Figure 5.- Aerodynamic characteristics of the plain wing and the cambered, twisted wing. R, 8 million.

Page intentionally left blank

Page intentionally left blank

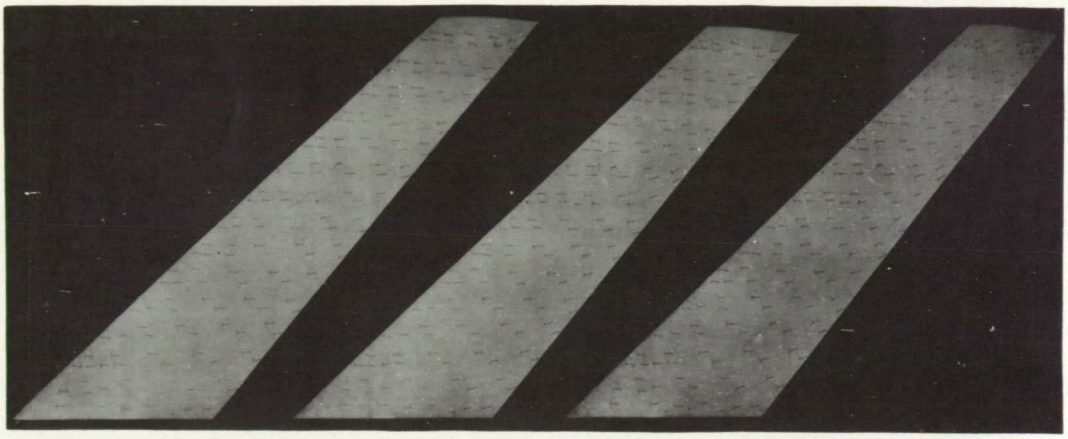

C_L,0.36 C_L, 0.65 C_L, 0.71

α, 6.1° α, 11.2° α, 12.2°

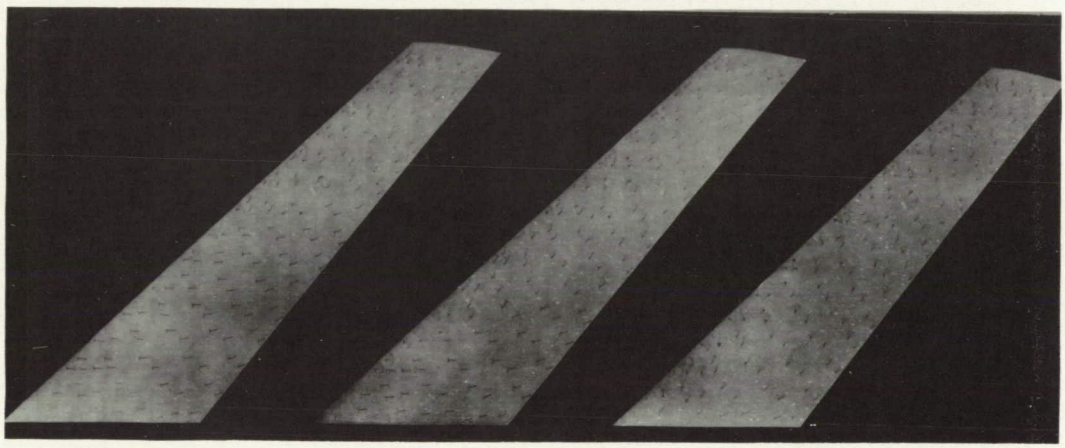

C_L, 0.80 C_L, 0.82 C_L, 0.94

α, 14.2° α, 15.2° α, 24.3°

NACA
A-14619

(a) Plain wing.

Figure 6.– Tuft photographs of the stalling behavior on the wing models at a Reynolds number of 8 million.

Page intentionally left blank

Page intentionally left blank

C_L, 0.39 C_L, 0.72 C_L, 0.93

α, 6.1° α, 12.2° α, 16.3°

C_L, 1.07 C_L, 1.09 C_L, 1.07

α, 20.3° α, 21.3° α, 22.3°

NACA
A-14620

(b) Cambered, twisted wing.

Figure 6.– Concluded.

Page intentionally left blank

Page intentionally left blank

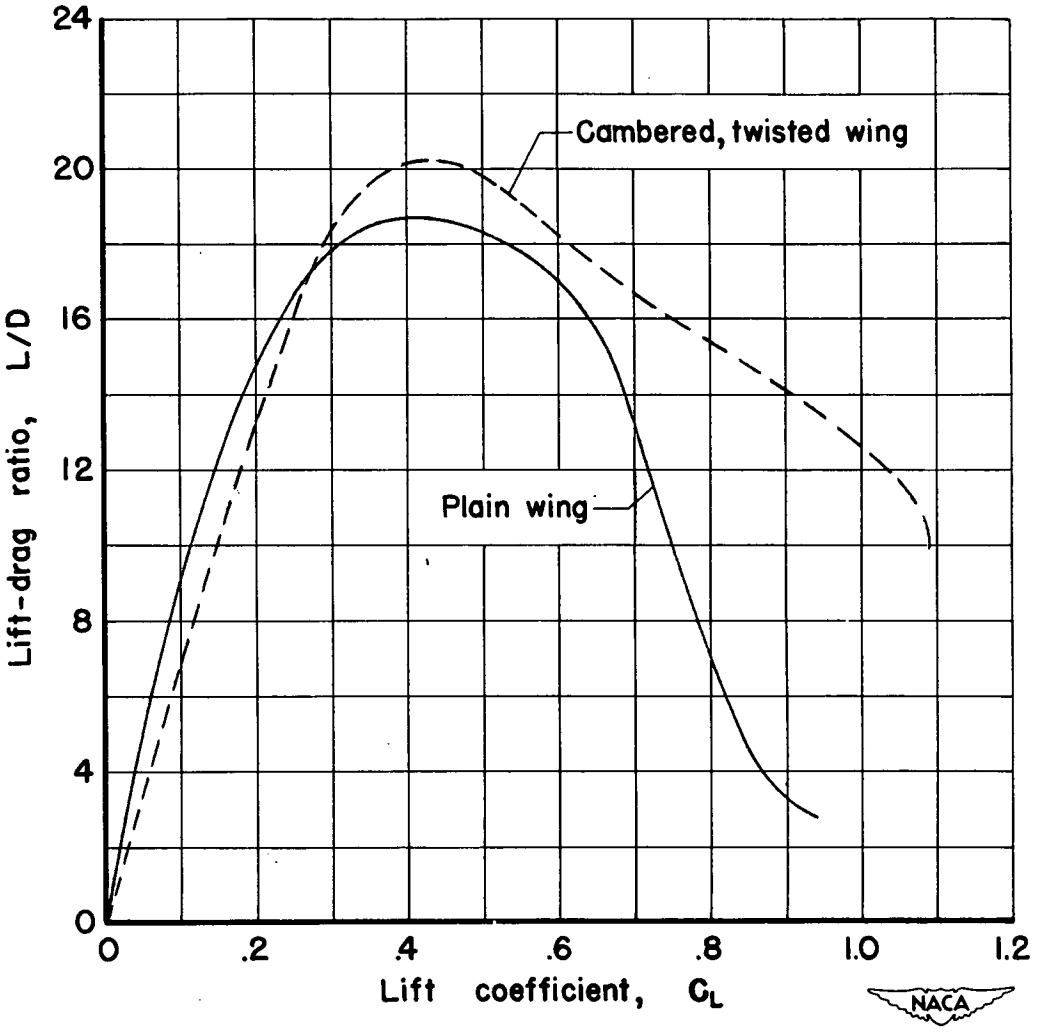

Figure 7.- Comparison of the lift-drag ratio characteristics for the plain wing and the cambered, twisted wing.

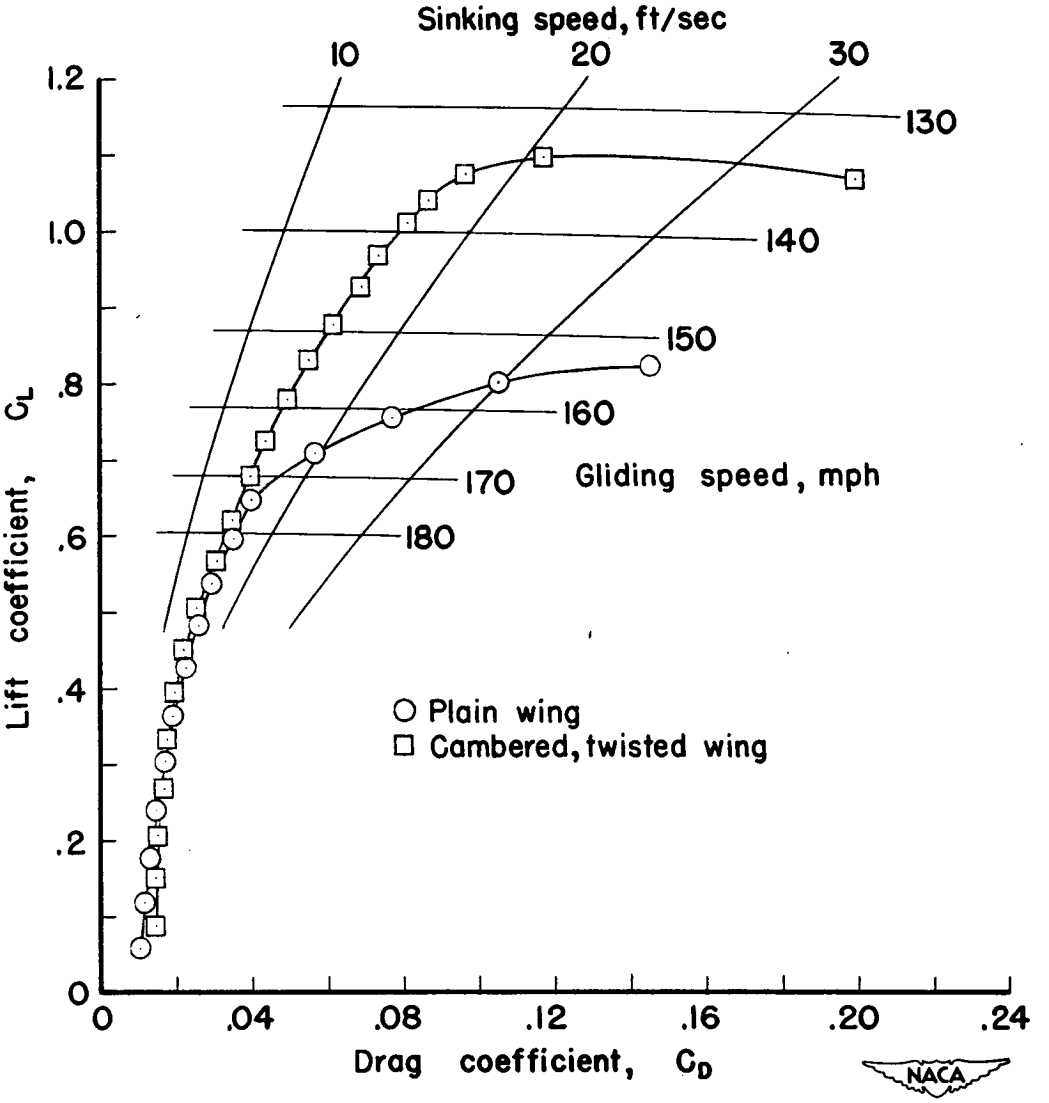

Figure 8.- Comparison of the power-off gliding characteristics for the plain wing and the cambered, twisted wing. Wing loading, 50 pounds per square foot.

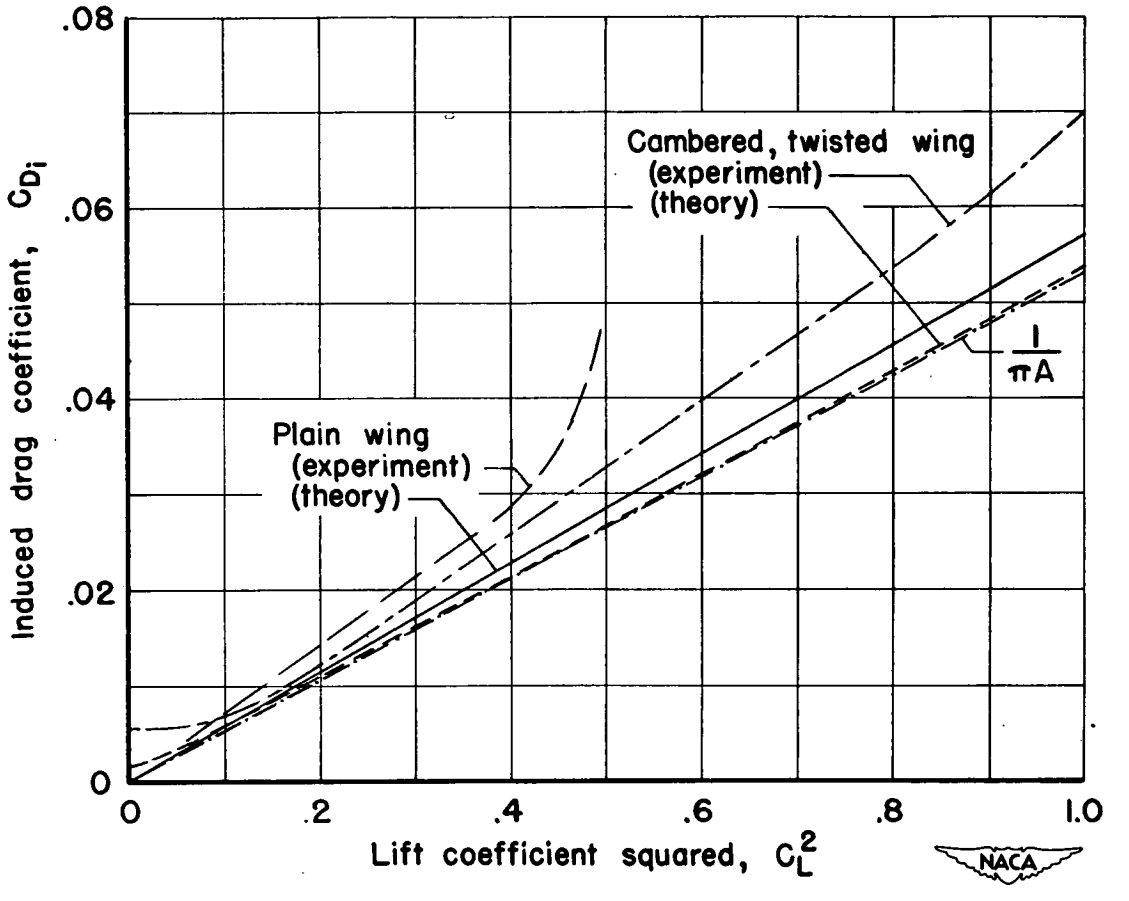

Figure 9.- Comparison of the theoretical and experimental induced-drag characteristics of the plain wing and the cambered, twisted wing.

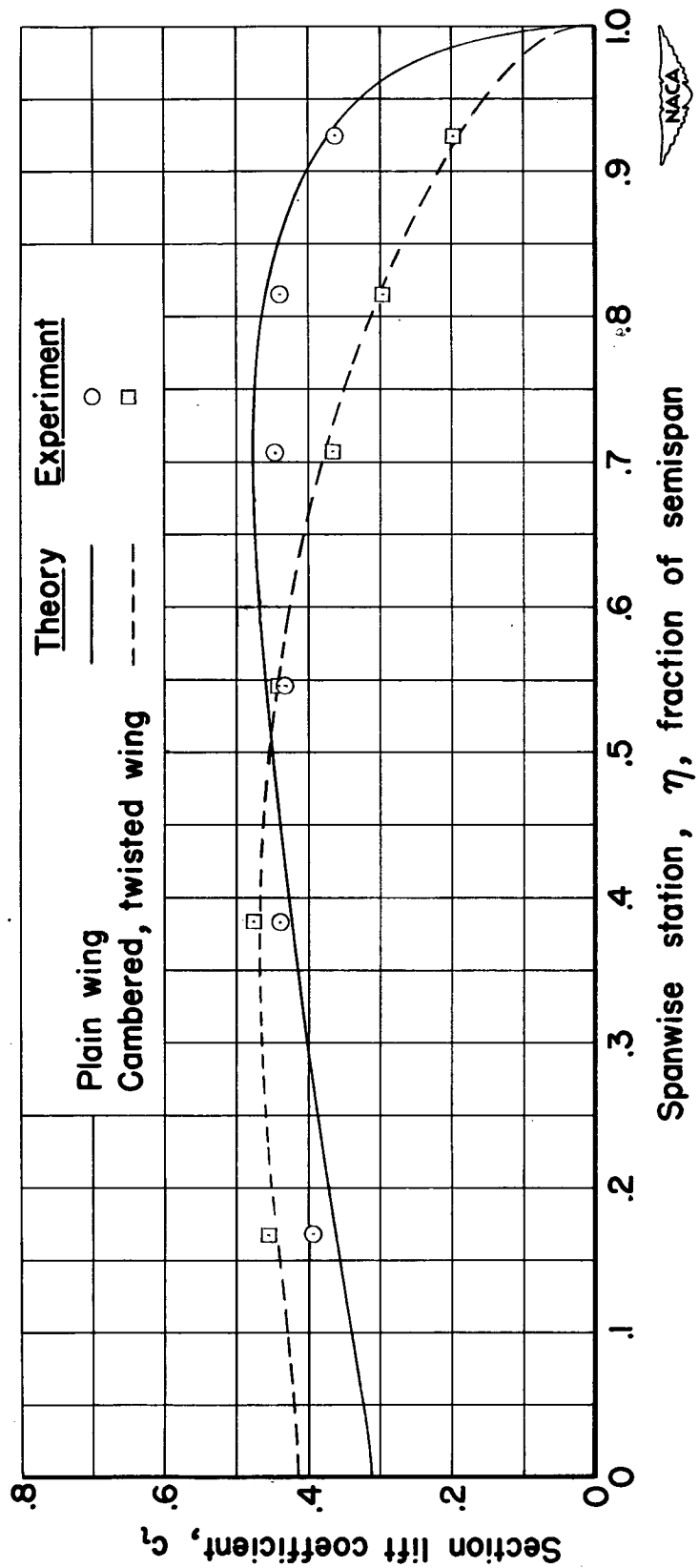

Figure 10.- Comparison of the theoretical and experimental spanwise distribution of section lift coefficient for the plain wing and the cambered, twisted wing at a lift coefficient of 0.4.